



**HAL**  
open science

# A level-set framework for the wind turbine wake analysis: from high-fidelity unsteady simulations to 1D momentum theory

Félix Houtin-Mongrolle, Pierre Bénard, Ghislain Lartigue, Vincent Moureau

► **To cite this version:**

Félix Houtin-Mongrolle, Pierre Bénard, Ghislain Lartigue, Vincent Moureau. A level-set framework for the wind turbine wake analysis: from high-fidelity unsteady simulations to 1D momentum theory. *Journal of Physics: Conference Series*, 2021, 1934 (1), pp.012011. 10.1088/1742-6596/1934/1/012011 . hal-03254788

**HAL Id: hal-03254788**

**<https://hal.science/hal-03254788>**

Submitted on 26 Jul 2021

**HAL** is a multi-disciplinary open access archive for the deposit and dissemination of scientific research documents, whether they are published or not. The documents may come from teaching and research institutions in France or abroad, or from public or private research centers.

L'archive ouverte pluridisciplinaire **HAL**, est destinée au dépôt et à la diffusion de documents scientifiques de niveau recherche, publiés ou non, émanant des établissements d'enseignement et de recherche français ou étrangers, des laboratoires publics ou privés.

PAPER • OPEN ACCESS

## A level-set framework for the wind turbine wake analysis: from high-fidelity unsteady simulations to 1D momentum theory

To cite this article: F. Houtin—Mongrolle *et al* 2021 *J. Phys.: Conf. Ser.* **1934** 012011

View the [article online](#) for updates and enhancements.

 <p>The Electrochemical Society Advancing solid state &amp; electrochemical science &amp; technology 2021 Virtual Education</p> <p><b>Fundamentals of Electrochemistry:</b> Basic Theory and Kinetic Methods Instructed by: <b>Dr. James Noël</b> Sun, Sept 19 &amp; Mon, Sept 20 at 12h–15h ET</p> <p>Register early and save!</p>	
--	--

# A level-set framework for the wind turbine wake analysis: from high-fidelity unsteady simulations to 1D momentum theory

F. Houtin–Mongrolle<sup>1</sup>, P. Benard<sup>1</sup>, G. Lartigue<sup>1</sup>, V. Moureau<sup>1</sup>

<sup>1</sup>Normandie Univ, INSA Rouen, UNIROUEN, CNRS, CORIA, Rouen 76000, France

E-mail: felix.houtin-mongrolle@coria.fr

February 2021

**Abstract.** In the context of yawed wind turbine wakes, the validity of the so-called 1D momentum theory is arguable. The 1D momentum theory emerges from an inviscid, steady and irrotational analysis of the streamtube surrounding a wind turbine while the wake aerodynamics under yaw is modified. In this work, the mean flow streamtube around a single DTU 10MW wind turbine, under yaw misalignment and turbulent inflow is investigated with Large-Eddy Simulation combined to the Actuator Line method. The simulations are performed on a highly resolved grid counting billions of elements. The streamtube construction from the mean flow is based on the transport of accurate conservative level set functions. Integration of local flow quantities within the streamtube presents similarities when the streamtube expansion occurs past the turbine until the velocity deficit starts to recover. Mean kinetic energy and momentum budget are then presented to explain the yawed wake recovery and deflection process. Background turbulence plays a key role in the recovery process while the deflection of the wake is impacted by pressure forces on the streamtube. From these budgets, four wake regions showing similar flow dynamics are defined and correlated to local flow structures.

*Keywords:* Large Eddy Simulation, Actuator Line Method, Yawed Wakes, Budget, Streamtubes

## 1. Introduction

Yaw control strategies have become an attractive approach to maximize the generated electrical power output of offshore wind farms. The wake deviation resulting from yawed turbines offers the possibility to reduce wake interactions within a wind farm and hence to reduce the associated power losses [1]. However, the yawed turbine aerodynamics is modified and leads to conditions out of the validity range of engineering wake models. Since experimental investigations on actual wind farms are difficult to carry out and given the constant growth of computational resources, high-order numerical simulations tend to be a promising approach [2].

High-fidelity unsteady flow simulations based on the actuator line method (ALM) [3] are becoming a state-of-the art tool to better predict and understand wind turbine wakes. Such simulations require a high spatial resolution, leading to meshes counting tens of million up to several billion cells. With the tremendous amount of generated data, the analysis is therefore



difficult. Nonetheless, these simulations should help understanding the wake behavior and eventually improve reduced engineering models [4; 5] based on 1D momentum theory [6].

This work aims at investigating the wake of a yawed wind turbine under uniform and turbulent inflow using Large-Eddy Simulation (LES). The wake analysis is based on the construction of a streamtube [7] surrounding the turbine obtained via Level Set functions [8] transported by the time-averaged flow. Four cases are investigated with different yaw misalignment and inflow turbulence conditions. First, global quantities are integrated over the streamtube sections. Variations of velocity, pressure and turbulent kinetic energy allow to draw connections between the mean flow behavior explained through 1D momentum theory and the highly resolved flow dynamics. This analysis seeks to complete the already observed flow deflection downstream yawed wind turbine [9]. Then, an analysis based on mean kinetic energy (MKE) and mean momentum (MM) budgets is performed. The MKE budget terms are associated to the wake destabilization process depending on the inflow turbulence. The deflection of the wake is finally investigated through the MM transport terms projected on the horizontal axis.

## 2. Numerical Framework

The filtered Navier–Stokes equations for constant density flows read:

$$\frac{\partial \tilde{u}_j}{\partial t} + \frac{\partial \tilde{u}_i \tilde{u}_j}{\partial x_i} = \nu \frac{\partial^2 \tilde{u}_j}{\partial x_i \partial x_i} - \frac{\partial \tau_{ij}^r}{\partial x_i} - \frac{1}{\rho} \frac{\partial \tilde{P}}{\partial x_j} + \tilde{f}_j \quad \text{and} \quad \frac{\partial \tilde{u}_i}{\partial x_i} = 0. \quad (1)$$

The truncation operator, which consists in projecting a field onto the LES grid, is written as  $\tilde{\bullet}$ . Using the Einstein summation convention,  $u$  is the fluid velocity vector,  $P$  is the hydrodynamic pressure,  $\nu$  is the kinematic viscosity of the fluid,  $\rho$  is the fluid density and  $f$  the volume forces. The subgrid scale stress tensor  $\tau_{ij}^r$  is based on the Dynamic Smagorinsky model [10].

This set of equations is integrated using the YALES2 flow solver [11]. YALES2 is a massively-parallel finite-volume solver, which is specifically tailored for Large-Eddy Simulation, and relies on a central 4th-order numerical scheme for spatial discretization, and a 4th-order Runge-Kutta like method [12] for the time integration on unstructured grid. Benard et al. [13] have shown the necessity of fairly high order numerics to ensure the proper transport of fine vortical structures present in wind turbine wakes in the context of ALM.

### 2.1. Wind turbine modelling

In this work, the modelled wind turbine is the academic DTU10MW [14]. This turbine follows the technological evolution of offshore wind turbines, reaching today hundreds of meters diameters. In the following, all quantities are scaled by the wind turbine diameter  $D = 178.3$  m and the free-stream velocity  $u_{\text{ref}} = 10$  m/s. The blades use multiple airfoils along the span with variable chord and twist [14]. The deformation of the blades are not taken into account in this study, which implies a strong hypothesis on the loads computation. Indeed, for such diameters the flapwise blade deformation at the tip can reach up to tens of meters [15]. With this hypothesis, the authors choose to use the non-prebended blades with the designed cone angle of  $2.5^\circ$ . The rotation speed is imposed to obtain the design tip speed ratio  $\lambda_{\text{opt}} = 7.5$ , giving a Reynolds number of approximately  $Re_{\text{tip}} \approx 6 \times 10^6$  at the blade tip. No control is applied and the pitch angle is kept to zero as the operating point lays in the first control region. The rotor blades are modelled as actuator lines which compute the blade forces at each time step based on the inflow velocity, the angle of attack  $\alpha$  and the chord-based Reynolds number lift  $C_L$  and drag  $C_D$  coefficients obtained from the airfoil properties [14]. After the computation of lift and drag forces  $\mathbf{F}_{2D} = (\mathbf{L}, \mathbf{D})$  at the ALM location using two-dimensional airfoil theory, the blade forces are regularized on the Eulerian grid by performing a convolution using an isotropic three-dimensional Gaussian kernel [3]. In such model, the unsteady force distribution of a blade

Case	$\gamma$	inflow	# elements	$\langle C_P \rangle \pm C_P'$	$\langle C_T \rangle \pm C_T'$
LY0	$0^\circ$	uniform	$1.9 \times 10^9$	$0.466 \pm 0.003$	$0.772 \pm 0.002$
LY30	$+30^\circ$	uniform	$1.7 \times 10^9$	$0.366 \pm 0.006$	$0.606 \pm 0.003$
TY0	$0^\circ$	$TI_{-2D} = 14\%$	$1.9 \times 10^9$	$0.49 \pm 0.09$	$0.78 \pm 0.07$
TY30	$+30^\circ$	$TI_{-2D} = 14\%$	$1.7 \times 10^9$	$0.39 \pm 0.08$	$0.62 \pm 0.06$

**Table 1.** Cases and mesh properties. Reference values for a laminar inflow are  $\langle C_P \rangle = 0.476$  and  $\langle C_T \rangle = 0.814$  [14].

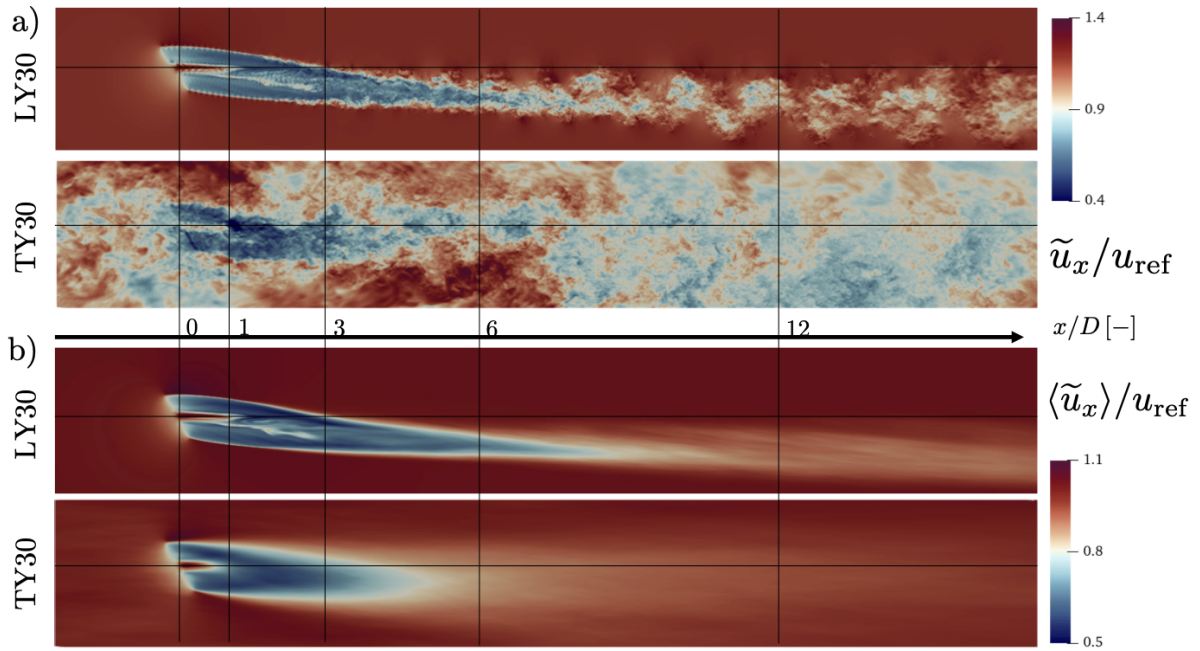


**Figure 1.** Horizontal slices at  $z/D = 0$  of (a) instantaneous streamwise velocity and (b) mean streamwise velocity for cases LY30 and TY30. The full domain is not represented,  $x/D \in [-2.5; 18.0]$  and  $y/D \in [-2.0; 1.0]$ .

on the flow is prescribed instead of being resolved by the flow solver. Each blade is discretized using 75 sections, i.e 75 points per actuator lines.

## 2.2. Cases description

The computational domains dimensions are  $L_x \times L_y \times L_z = 25D \times 10D \times 10D$ . The turbine is centred at  $5D$  from the inlet. Such dimensions allow to properly study the far wake and to prevent confinement effect due to the boundary proximity. Four cases are investigated in this work, two yaw angles ( $\gamma = 0^\circ, +30^\circ$ ) and two inflows (with and without turbulence), see Tab. 1 for the turbine performances of each cases. Special attention was paid to have a homogeneous cell size,  $D/\Delta = 162$ , in the wake and upstream the turbine, whether the turbine is yawed or under turbulence by using pre-computation and streamtube volumes to refine the mesh in the proper area. This part is not discussed further in this paper for the sake of brevity. The obtained meshes gather billions of elements, see Tab. 1. The injected turbulence is generated using the Mann algorithm [16].

Figure 1 presents a horizontal slice of the instantaneous and time-averaged streamwise velocity fields for cases LY30 and TY30. Temporal statistics, denoted with  $\langle \bullet \rangle$ , are averaged over 100  $D/u_{\text{ref}}$ . The instantaneous velocity fields present a wide range of turbulent scales, from tip

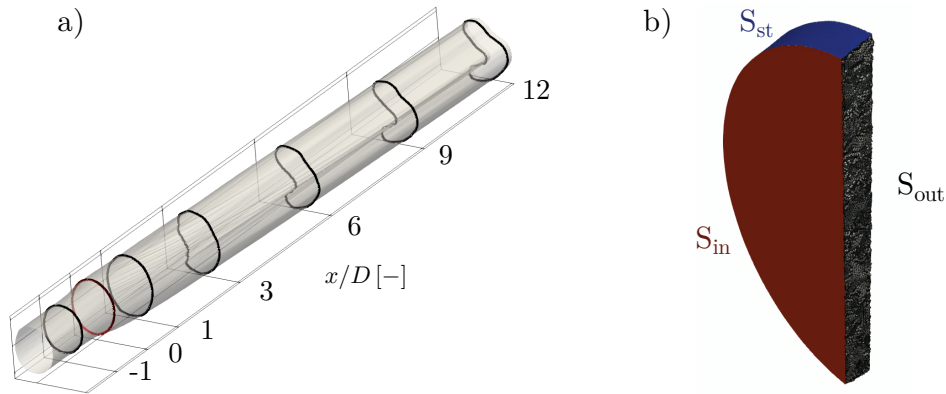


**Figure 2.** (a) Streamtube surface of the TY30 case based on the level set position, various streamwise slices are represented by bold lines (b) Half of a streamtube slice, picturing the considered surfaces and volume for data integration.

vortices being convected (LY30) to wake meandering (TY30).

### 2.3. Stream tube and Level Set functions

With the tremendous amount of data resulting from LES simulations, one should be able to retrieve the wake bounding of a wind turbine. Depending on the turbine alignment with the wind or the inflow, the wake bounding will change. The definition of a closed control volume surrounding the turbine allows to retrieve global quantities [17; 18], i.e. integrated data, compacting the relevant information to understand the wake physics. A volume based on streamtubes have shown interesting physical properties [19; 20] and can be defined around the turbine. The construction of a streamtube is based on the time averaged quantities and aims to represent the mean path of flow particles emanating from an upstream position. In this work, streamtubes are generated using Accurate Conservative Level Set (ACLS) [8] functions. Such functions are commonly used for two phase flow simulations in order to track a liquid-gas interface while remaining strictly conservative and with low diffusion errors [21]. The ACLS function is set to be a hyperbolic tangent profile where the interface is located at the iso-level 1/2. Here, the level set initialization is based on the mean regularized forces of the wind turbine on the eulerian grid, ensuring that all the modelled wind turbine forces are within the streamtube. In the ACLS function, a scalar  $\psi$  is advected according to the following equation:

$$\frac{\partial \psi}{\partial \tau} + \frac{\partial \psi \langle \tilde{u}_i \rangle}{\partial x_i} = 0 \quad (2)$$

where  $\tau$  is a pseudo time used to propagate the ACLS function. The streamtube is considered converged when the overall domain integral reaches a convergence factor  $\frac{\partial \psi}{\partial \tau} < \epsilon$ . Thanks to the free divergence of velocity, this ensures the correct streamtube property  $\langle \tilde{u}_i \rangle \frac{\partial \psi}{\partial x_i} \approx 0$ . The streamtube integrals are then obtained by triangulating the streamtubes faces as depicted on Fig. 2(a). Streamwise volume slices, see Fig. 2(b), of the streamtube are then used to study the evolution of the wake quantities. The exterior streamtube section surface is noted  $S_{st}$ , the upstream face is  $S_{in}$ , the downstream face  $S_{out}$  and the volume  $V_{st}$ . Integrals averaging, either on volume or surface, are denoted with  $\langle \bullet \rangle_S$ ,  $S$  being the corresponding surface or volume. For all cases  $\epsilon D/u_{ref} = 1.783 \times 10^{-4}$  and the dot product  $\langle \langle \tilde{u}_i \rangle n_i / \| \langle \tilde{u} \rangle \| \rangle_{S,st}$  remains below 0.6%. Therewith, the streamtube surface normal is considered orthogonal to the the local mean filtered

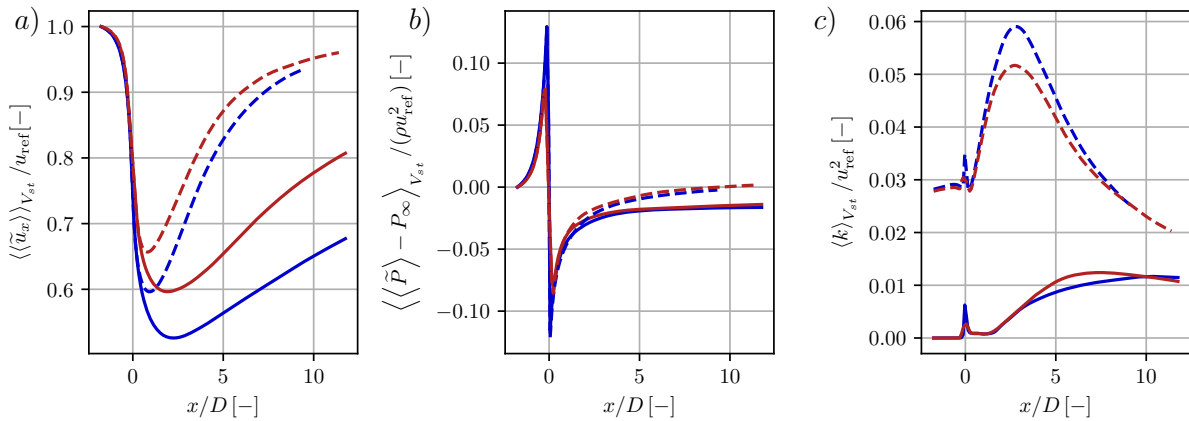


**Figure 3.** Streamwise evolution of (a) mean streamwise filtered velocity (b) hydrodynamic pressure and (c) turbulent kinetic energy integrated over the streamtube volume for cases LY0 (—), LY30 (—), TY0 (---) and TY30 (---).

velocity. The streamtubes are computed from  $2D$  upstream to  $12D$  downstream the turbine and discretized into 150 cross-sections of approximately 20 mesh cells thickness.

### 3. 1D momentum theory from streamtube data

In order to understand the yawed wake behavior, quantities of interest are averaged over control volume cross-sections, using the streamtubes control volume presented in section 2.3. Figure 3 shows the evolution of streamwise velocity, pressure and mean turbulent kinetic energy (TKE) for each case. TKE is defined as  $k = 1/2 \langle \tilde{u}_i'^2 \rangle$ , with  $\bullet' = \bullet - \langle \bullet \rangle$  being the temporal fluctuation operator. These quantities can be compared to the 1D momentum theory, which considers a one-dimensional velocity and pressure within the streamtube. The pressure drop is located at the turbine position when the flow decelerates as a consequence of the turbine momentum extraction from the flow. For yawed cases, inducing a lower thrust coefficient, the velocity deficit and the pressure difference are lower. For cases with turbulent injection, half of the deficit is restored after  $4.5D$  downstream the turbine. Without turbulence, the deficit takes at least twice this length to recover, demonstrating the major role of turbulence on the velocity deficit recovery. The TKE evolution also gives information on the wake recovery dynamics. For uniform inflow cases, a plateau can be observed up to  $1.5D$  behind the rotor followed by an increase of TKE. This variation of TKE is precisely located at the maximum velocity deficit position. Figure 4 depicts the streamtube cross section area, its center and the horizontal mean velocity evolution along the axial axis. As the streamtube volume is mass-conserving, the cross section area change is directly linked to the previous observations on the velocity deficit. When the streamtube approaches the turbine, its section expands until the maximum velocity deficit is reached while its section shrinks when the wake starts to recover. This last part differs from the classical streamtube analysis where only an upstream and downstream cross-section/velocity state are considered [6], the velocity deficit recovery is not included in this theory.

The wake center deflection represents one of the main features of a yawed wind turbine. The case without turbulence is less deflected after  $5D$  downstream the turbine. The analysis of Bastankhah and Porté-Agel [9] based on experimental results is contradictory at first glance, presenting that a decrease in the incoming turbulence intensity is found to increase wake deflection for a yawed turbine. Yet the computed deflection here is based on the mean streamtube center while it is based on the maximum velocity deficit position in [9]. It is qualitatively visible in Fig. 1(b) that the maximum velocity deficit is less deflected for the turbulent case. The

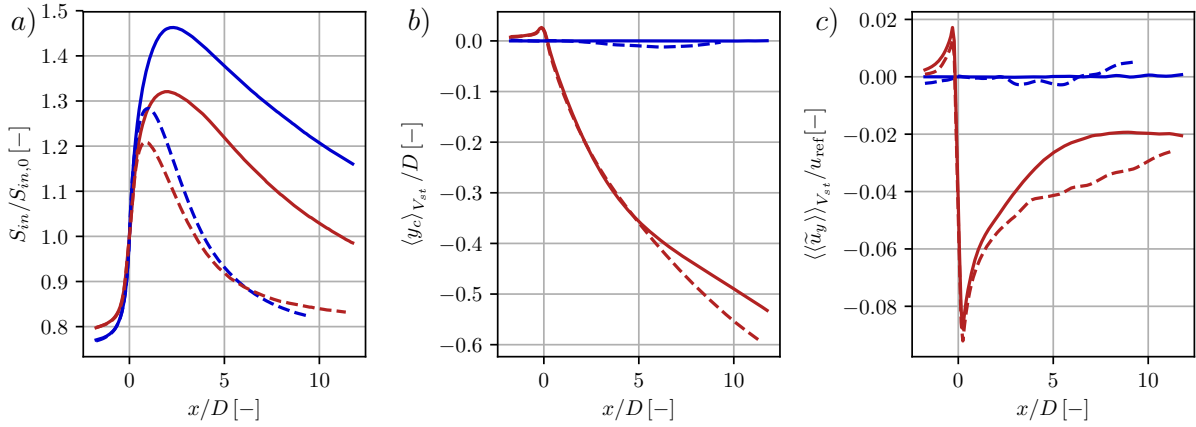


**Figure 4.** Streamwise evolution of (a) the streamtube sectional area,  $S_{in}$  normalized by the section at the rotor position, (b) the streamtube center in the transverse plane direction (c) the horizontal mean velocity. Cases LY0 (—), LY30 (—), TY0 (---) and TY30 (---).

horizontal velocity is directly linked to the streamtube center deflection. At the turbine position, the local mean velocity goes from positive to negative values which implies a redirection of the flow and will be further discussed in section 5.

#### 4. Turbulence impact on Mean Kinetic Energy budget

To quantify the wake destabilisation process and wake recovery, mean kinetic energy (MKE) budgets are performed. The MKE transport equation are derived from equation (1) by multiplying them with  $\langle \tilde{u}_i \rangle$ . Then, terms are decomposed as time-averaged and resolved fluctuations and integrated over streamtube cross-sections, giving:

$$\begin{aligned} \oint_S \left( \underbrace{\frac{1}{2} \rho \langle \tilde{u}_i \rangle \langle \tilde{u}_i \rangle \langle \tilde{u}_j \rangle}_{i} + \underbrace{\langle \tilde{u}_j \rangle \langle \tilde{P} \rangle}_{ii} + \underbrace{\langle \tilde{u}_i \rangle \rho \langle \tilde{u}'_i \tilde{u}'_j \rangle}_{iii} + A_{j,S} \right) n_j dS \\ - \iiint_{V_{st}} \left( \underbrace{\rho \langle \tilde{S}_{ij} \rangle \langle \tilde{u}'_i \tilde{u}'_j \rangle}_{iv} + \underbrace{\rho \langle \tilde{u}_i \rangle \langle \tilde{f}_i \rangle}_{v} + A_V \right) dV = 0, \end{aligned} \quad (3)$$

with  $\langle \tilde{u}'_i \tilde{u}'_j \rangle$  denoting the Reynolds stress tensor and  $\tilde{S}_{ij} = \frac{1}{2} \left( \frac{\partial \tilde{u}_i}{\partial x_j} + \frac{\partial \tilde{u}_j}{\partial x_i} \right)$  the strain rate tensor. Viscous and subgrid scale terms, on the surface and in the volume, are gathered as  $A_S$  and  $A_V$ , respectively, and are further ignored in the analysis since they are negligible at such high Reynolds numbers, but are correctly taken into account in the budget residual. Numbered terms respectively denotes: *i*) the change in flux of MKE by advection, *ii*) the pressure work, *iii*) the work of the Reynolds stress tensor on the streamtube surfaces, *iv*) the production of TKE within the streamtube volume and *v*) the work of the turbine.

This integrated budget is shown on Fig. 5, comparing the yawed wind turbine cases TY30(a) and LY30(b). One of the major contribution to the MKE budget is the turbine work, generating the first energy drop. It is counter balanced by the pressure and advection of MKE, therewith being the first source of MKE. Afterwards, the wake can be decomposed in different regions, denoted *I*, *II*, *III* and *IV*. The first, appearing only for LY30, is the vortex advection region. In this region the tip vortices remain helical until  $1.5D$  downstream. The first vortices instabilities appear in the streamwise direction. The second region starts with the production of TKE,

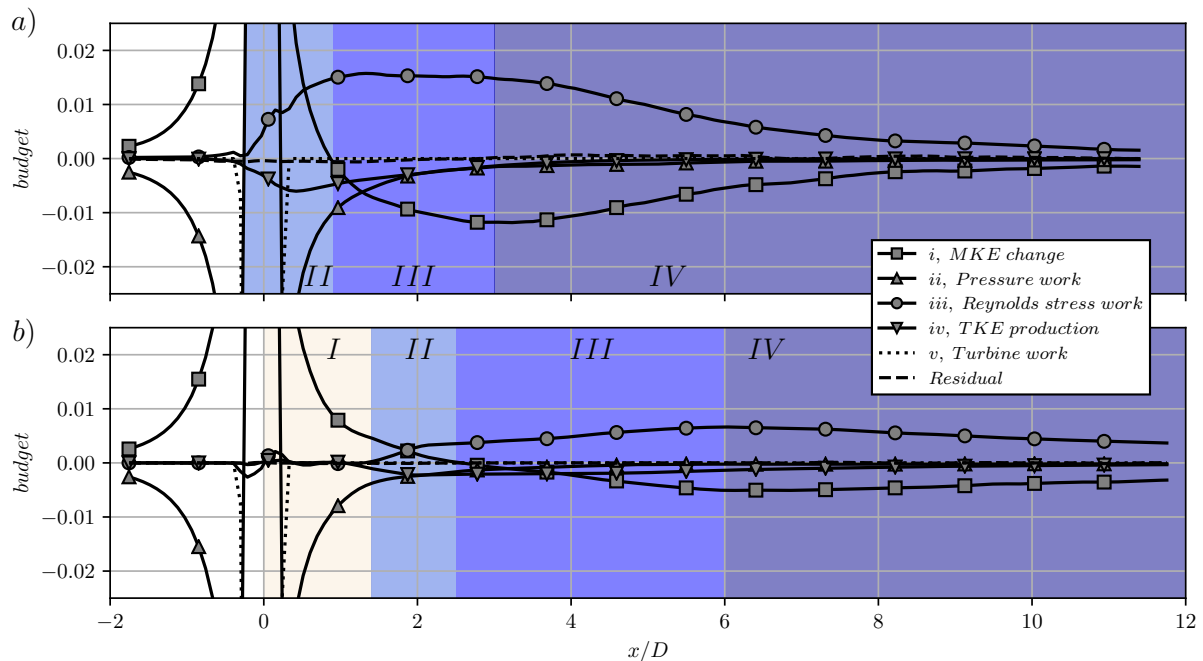


**Figure 5.** Mean kinetic energy equation terms integrated over the streamtube cross-section for cases TY30(a) and LY30(b). Each term is normalized by the total turbine power such as the integral of **term**  $v$  is equal to -1. The residual corresponds to the sum of all terms of equation (3).

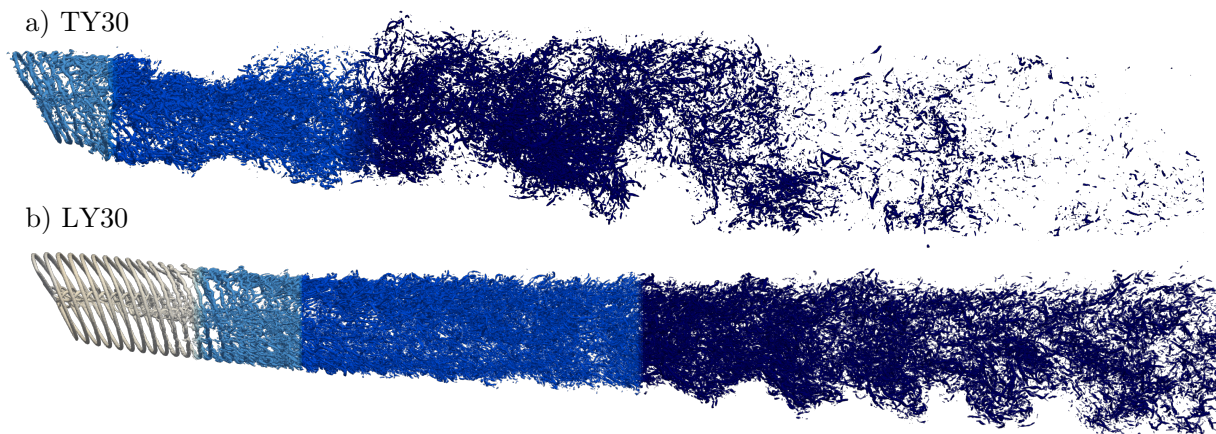


**Figure 6.** 3D visualisation of the instantaneous Q-criterion colored by the regions determined from the MKE budgets for cases TY30 and LY30.

removing energy from the mean (also observed on Fig. 3(c)). The Reynolds stress work balances this production by supplying energy to the streamtube. The tip vortices pairs up to each other in this region, or interact with background turbulence generating a TKE production peak. The third region is delimited by the MKE advection becoming negative in the wake until it begins to increase again. Here, the wake velocity deficit starts to recover due to the large Reynolds stress contribution. From Fig. 3(c) the end of this region presents the maximum of turbulent kinetic energy. The last identified region contains the wake turbulence decaying. Turbulence production becomes negligible and the Reynolds stress work decreases significantly. The velocity

deficit continues to recover but at a lower rate than the previous region. Figure 6 pictures the 3D iso-contour of  $Q$ -criterion for both cases, colored by the different regions presenting the vortex dynamics. Similar regions are observed for LY0 and TY0, but not presented here for the sake of brevity. The only point is that region *III* ends further downstream for LY0 (9D) compared to LY30 (6D). This last point implies a slower wake recovery for the unyawed case under uniform inflow, which is not observed with the turbulent cases. Yet comparing the four cases, the background turbulence plays a large role in the wake dynamics as mentioned in the literature [20; 22].

### 5. Yaw impact on Mean Momentum budget

Mean momentum transport equations are used to understand the wake deflection of the turbine under yaw misalignment. Decomposing Eq. (1) terms into time-averaged and resolved fluctuations, integrating them over a streamtube cross-section and projecting the terms onto the streamwise and horizontal axis gives, respectively:

$$\oint_S \left( \underbrace{\langle \tilde{u}_x \rangle \langle \tilde{u}_j \rangle n_j}_i + \underbrace{\frac{1}{\rho} \langle \tilde{P} \rangle n_x}_{ii} + \underbrace{\langle \tilde{u}'_x \tilde{u}'_j \rangle n_j}_{iii} + A_x \right) dS - \iiint_{V_{st}} \underbrace{\langle \tilde{f}_x \rangle}_{iv} dV = 0, \quad (4)$$

$$\oint_S \left( \underbrace{\langle \tilde{u}_y \rangle \langle \tilde{u}_j \rangle n_j}_i + \underbrace{\frac{1}{\rho} \langle \tilde{P} \rangle n_y}_{ii} + \underbrace{\langle \tilde{u}'_y \tilde{u}'_j \rangle n_j}_{iii} + A_y \right) dS - \iiint_{V_{st}} \underbrace{\langle \tilde{f}_y \rangle}_{iv} dV = 0. \quad (5)$$

Similarly to Eq. (3), viscous and subgrid scale terms are gathered in  $A$  and are negligible, yet included into the budget residual. Numbered terms respectively denote: *i*) change in momentum, *ii*) pressure force, *iii*) forces due to Reynolds stress and *iv*) the turbine forces on the flow.

Figure 7 represents the mean momentum budget terms projected on the streamwise and horizontal axes for both laminar inflow cases. A region analysis similar to the one of the MKE budget can be performed with the projection on the streamwise axis: both cases show similar regions with region *IV* being delayed for LY0. The horizontal projection brings more useful data and a different behaviour appears. All LY0 case terms are negligible in this direction. With the LY30 case, a part of the forces are imposed in the horizontal direction and induces a drop in the horizontal momentum. As in the streamwise direction, this sink of momentum is counter-balanced by the pressure forces and the change in momentum. Note that when the change in momentum is negative (on the opposite, positive), horizontal velocity increases (decreases). The absolute value informs on the velocity change rate. In the LY30 case, since the change of momentum upstream the turbine is negative, the flow field is slightly reoriented in the horizontal direction (around  $1.0^\circ$ ). In region *I*, the momentum changes abruptly to positive values to counter the turbine forces and the horizontal flow direction changes to  $-8^\circ$ . Then the horizontal velocity starts recovering quickly. These comments on the horizontal velocity can be correlated to the streamtube center deflection (see Fig. 4(b-c)). In the second region, pressure forces drop due to Reynolds stress forces triggering the vortices pairing. A balance between the pressure term and the Reynolds stress was suggested in the experimental work of Bastankhah and Porté-Agel [9] but could not be measured. The momentum flux becomes constant, but remains almost negative and the horizontal velocity recovers linearly. In region *III*, MM terms are mainly constant. In the last region, all MM terms slightly tend to 0: the wake deflection direction is kept downstream.

### 6. Conclusions

Mean momentum and kinetic energy budgets were performed on wind turbine wake streamtubes constructed from high-fidelity LES. The advantage of this streamtube analysis strategy is double.

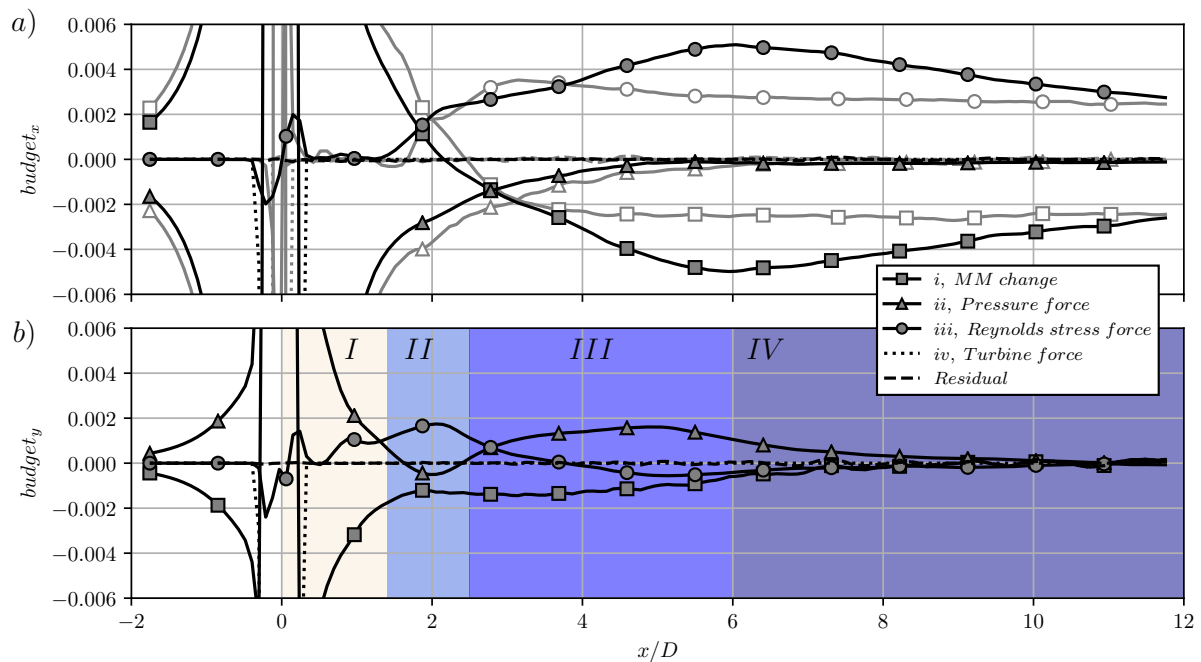


**Figure 7.** Mean momentum transport equation terms integrated over the streamtube cross-section and projected on (a) the streamwise (Eq. (4)) and (b) the horizontal axis (Eq. (5)), for cases LY0 (—) and LY30 (—). Each term is normalized by the total turbine forces such as the integral of term  $iv$  is equal to -1. The residual corresponds to the sum of all terms of the equations. The regions discussed in the previous section are colored on (b).

First, it allows to reduce the amount of information from high-fidelity simulation counting billions of elements. Secondly, the obtained results are comparable to classical 1D momentum theory for steady, inviscid and irrotational flows, which are at the basis of wake models for the design of modern wind turbines. Variations of yaw angle or turbulence inflow have shown a similar behavior of the streamtube averaged quantities compared to theory. Indeed, the streamtube expands as it approaches the turbine and a velocity deficit appears. For yawed turbine cases, the expected horizontal deviation of the streamtube center is observed. Moreover, the mean kinetic energy budget analysis showed that the wake recovers in different regions downstream the turbine. These regions are related to the local vortex structures in the vicinity of the turbine. The wake deflection induced by yawed turbine is explained through pressure forces and momentum fluxes in the mean horizontal momentum budget. Yet, to fully understand the wake behavior, an analysis of the instantaneous properties should be conducted. Indeed, the wake recovery understanding is highly dependent on the local energy fluxes and the wake boundary topology. This deeper analysis should help derive inputs for reduced wake models.

## 7. Acknowledgment

This work was granted access to HPC resources from TGCC, France through the PRACE project untitled "Wind Turbines Multi Physics" under the allocation 2020225444 and through GENCI, France under allocation A0082A11335 and from CRIANN, France, under the allocation 2012006.

## References

- [1] Gebrraad P M O, Teeuwisse F W, van Wingerden J W, Fleming P A, Ruben S D, Marden J R and Pao L Y 2016 *Wind Energy* **19** 95–114

- [2] Breton S P, Sumner J, Sørensen J N, Hansen K S, Sarmast S and Ivanell S 2016 *Philosophical Transactions of the Royal Society A: Mathematical, Physical and Engineering Sciences* **375** 20160097
- [3] Sørensen J and Shen W 2002 *J Fluids Eng* **124** 393–9
- [4] Zong H and Porté-Agel F 2020 *Journal of Fluid Mechanics* **889** A8
- [5] Porté-Agel F, Bastankhah M and Shamsoddin S 2020 *Boundary-Layer Meteorology* **174** 1–59
- [6] Sørensen J N 2016 *The general momentum theory* vol 4 (Springer)
- [7] Lebron J, Castillo L and Meneveau C 2012 *Journal of Turbulence* **13** 1–22
- [8] Desjardins O, Moureau V and Pitsch H 2008 *J Comput Phys* **227** 8395–416
- [9] Bastankhah M and Porté-Agel F 2016 *Journal of Fluid Mechanics* **806** 506–541
- [10] Germano M, Piomelli U, Moin P and Cabot W H 1991 *Physics of Fluids A: Fluid Dynamics* **3** 1760–5
- [11] Moureau V, Domingo P and Vervisch L 2011 *Comptes Rendus Mécanique* **339** 141–8
- [12] Kraushaar M 2011 *Application of the compressible and low-Mach number approaches to Large-Eddy Simulation of turbulent flows in aero-engines* Ph.D. thesis INPT
- [13] Benard P, Viré A, Moureau V, Lartigue G, Beaudet L, Deglaire P and Bricteux L 2018 *Computers & Fluids* **173** 133–9
- [14] Bak C, Zahle F, Bitsche R, Kim T, Yde A, Henriksen L C, Natarajan A and Hansen M 2013 DTU 10MW Reference Wind Turbine Tech. rep. DTU Wind Energy
- [15] Manolas D I, Pirrung G R, Croce A, Roura M, Riziotis V A, Madsen H A, Pizarro C, Voutsinas S G and Rasmussen F 2015 *European Wind Energy Association Annual Conference and Exhibition 2015, EWEA 2015 - Scientific Proceedings*
- [16] Mann J 1998 *Probabilistic Engineering Mechanics* **13** 269–82
- [17] Ge M, Gayme D F and Meneveau C 2021 *Renewable Energy* **163** 1063–77
- [18] Noca F, Shiels D and Jeon D 1999 *Journal of Fluids and Structures* **13** 551–78
- [19] Meyers J and Meneveau C 2013 *Journal of Fluid Mechanics* **715** 335–58
- [20] West J R and Lele S K 2020 *Energies* **13** 1–25
- [21] Janodet R, Guillamón C, Moureau V, Mercier R, Lartigue G, Benard P, Ménard T and Berlemont A 2020 (*Preprint* <https://hal.archives-ouvertes.fr/hal-03024186>)
- [22] Wu Y T and Porté-Agel F 2012 *Energies* **5** 5340–62